SUPPLEMENTARY INFORMATION

FGF21 Protects Against HFpEF by Improving Cardiac Mitochondrial Bioenergetics in Mice

Ke Zhang[1,8], Jing Gan[2,8], Baile Wang[3,8], Wei Lei[1,4,8], Dong Zhen[5], Jie Yang[6], Ningrui Wang[1], Congcong Wen[1], Xiaotang Gao[1], Xiaokun Li[1], Aimin Xu[3], Xinguang Liu[7*], Yulin Li[6*], Fan Wu[2*], Zhuofeng Lin[1,2*]

[1] School of Pharmaceutical Sciences, Wenzhou Medical University, Wenzhou 325035, China
[2] The Affiliated Dongguan Songshan Lake Center Hospital, the Innovative Center of Cardiometabolic Disease, Guangdong Medical University, Dongguan 523808, China
[3] State Key Laboratory of Pharmaceutical Biotechnology, the University of Hong Kong, Hong Kong 999077, China
[4] Affiliated Hospital of Guangdong Medical University, Zhanjiang 524001, China
[5] The Affiliated Hospital of Wenzhou Medical University, Wenzhou 325035, China
[6] Beijing Institute of Heart, Lung, and Blood Vessel Diseases, Anzhen Hospital of Capital Medical University, Beijing 100029, China
[7] Guangdong Provincial Key Laboratory of Medical Immunology and Molecular Diagnostics, Guangdong Medical University, Dongguan 523808, China
[8] These authors contributed equally: Ke Zhang, Jing Gan, Baile Wang, Wei Lei
*Correspondence: liuxg@gdmu.edu.cn; lyllyl_1111@163.com; zflwf@126.com; zlin@gdmu.edu.cn.

Supplementary Figure 1

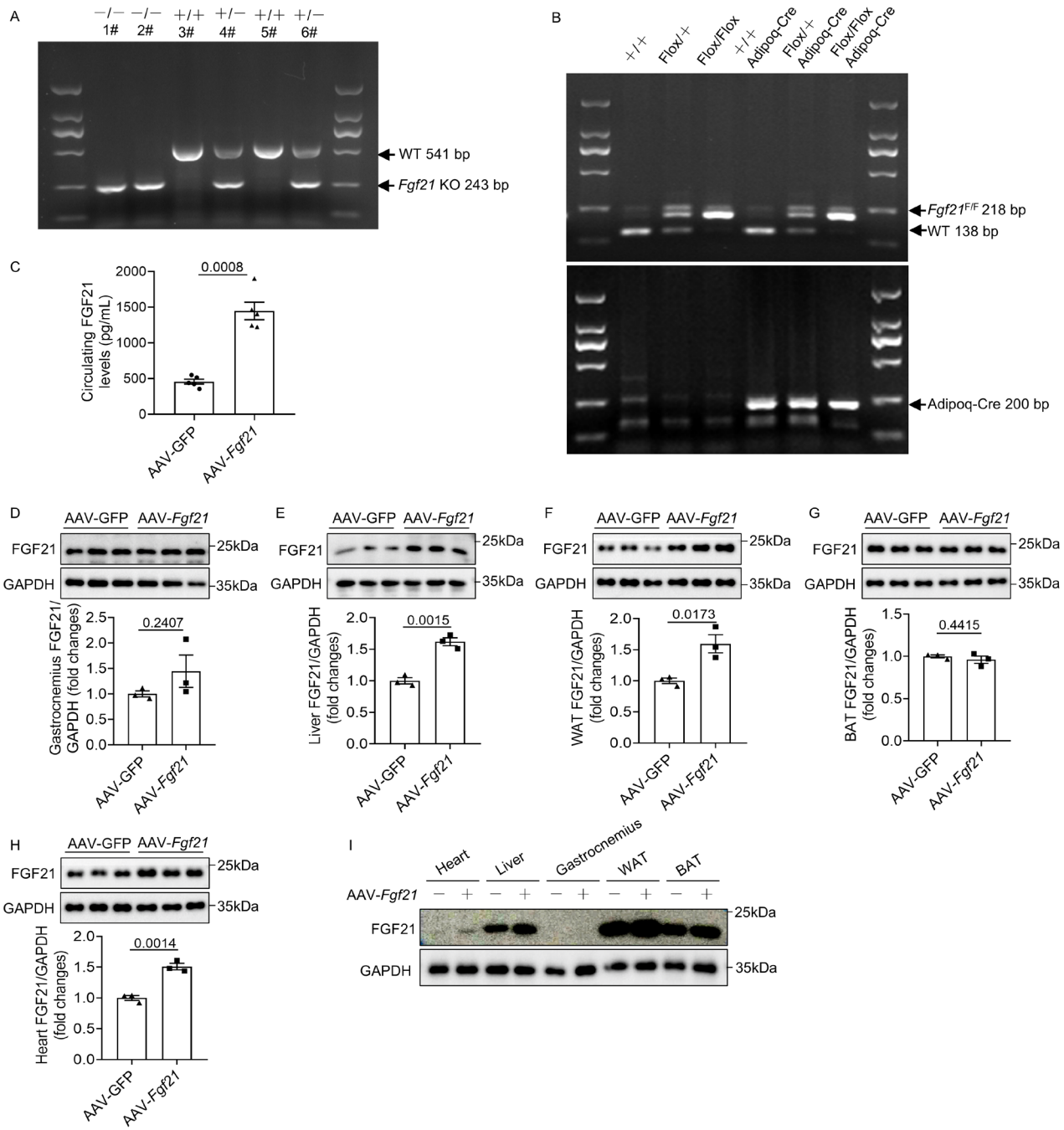

Supplementary Figure 1. Genotyping of FGF21 null mice and FGF21 levels in mice treated with AAV-*Fgf21*. **A** Representative polymerase chain reaction (PCR) genotyping of *Fgf21* KO and WT littermate mice. Genotypes of mice were determined by PCR using the following primers: P1-*Fgf21* (5'-GACTGTTCAGTCAGGGATTG-3'), P2-*Fgf21* (5'-CCCGTGATATTGCTGAAGAG-3') and P3-*Fgf21* (5'-ACAGGGTCTCAGGTTCAAAG-3'). The length of the PCR product of WT primers was 541 bp and *Fgf21* KO primers was 243 bp. **B** Representative PCR genotyping results. Genotyping primers for *Fgf21*$^{F/F}$ mice were described as follows: F1 (5'-TGTACCTGACCTAACCTCTCTCAG-3') and R1 (5'-CAGTGTCTTCCCTCAACTTTTCTC-3'). The length of the PCR product of WT primers was 138 bp and *Fgf21*$^{F/F}$ primers was 218 bp. Genotyping primers for Adipoq-Cre mice were described as follows: F1 (5'-GGATGTGCCATGTGAGTCTG-3') and R1 (5'-ACGGACAGAAGCAT

TTTCCA-3'). The length of PCR product of Adipoq-Cre primers was 200 bp. **C** Circulating levels of FGF21 at two weeks after treatment with AAV-*Fgf21* or AAV-GFP. $n = 5$ mice per condition. **D**-**H** FGF21 contents in gastrocnemius (**D**), liver (**E**), white adipose tissue (WAT, **F**), brown adipose tissue (BAT, **G**) and heart (**H**) of mice with HFpEF after treatment with AAV-*Fgf21* or AAV-GFP were tested by immunoblot, respectively. $n = 3$ mice per condition. **I** FGF21 contents in various organs of mice with HFpEF after treatment with AAV-*Fgf21* or AAV-GFP. $n = 3$ independent experiments. Data are represented as mean ± SEM. Statistical significance was determined by the two-tailed unpaired Student's *t* test with Welch's correction (**C**). Other assays were assessed by the two-tailed unpaired Student's *t*-test (**D**-**H**).

Supplementary Figure 2

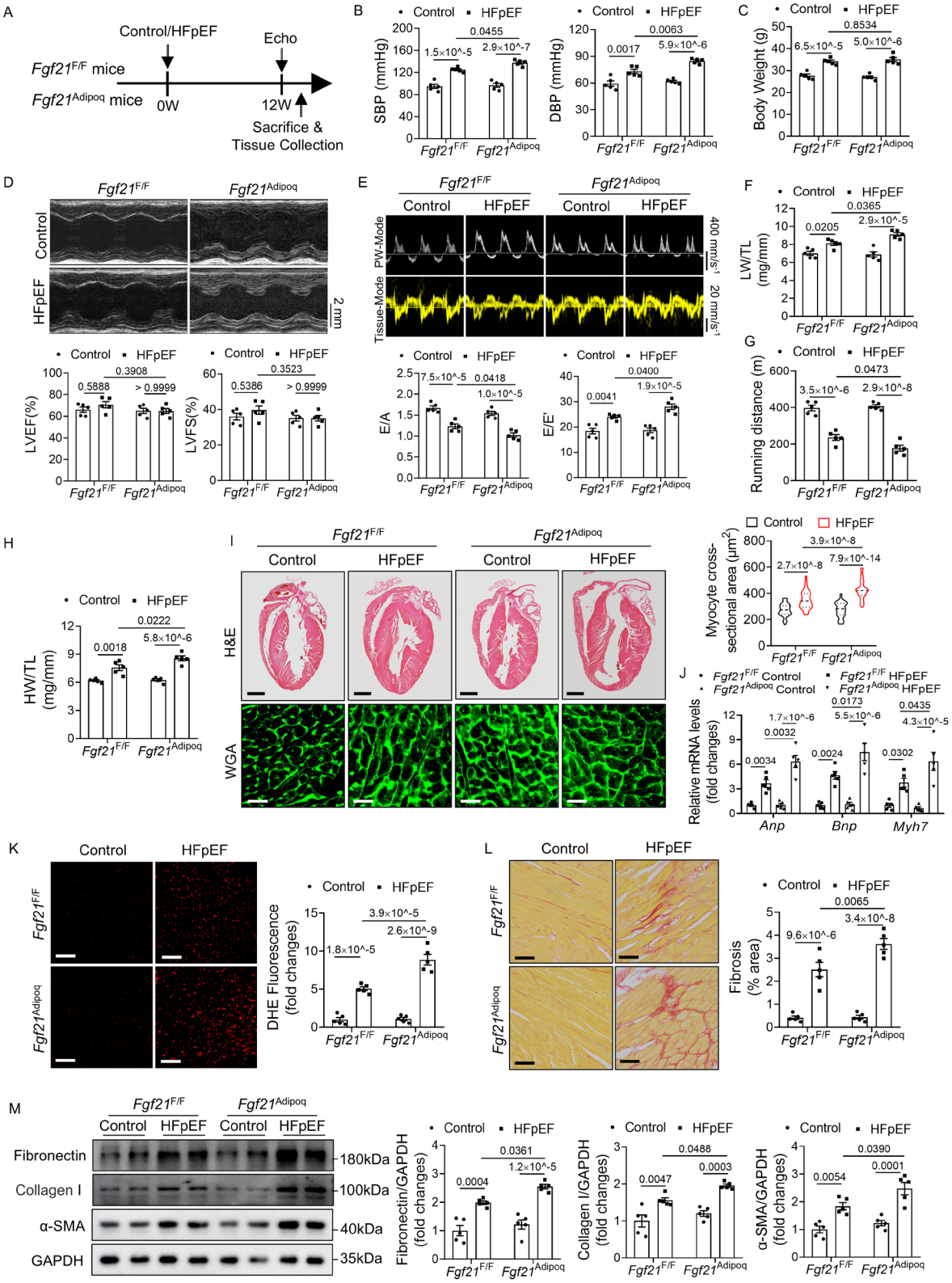

Supplementary Figure 2. Adipocytes-specific FGF21 deficiency decreases cardiac diastolic function and increases myocyte size, oxidative stress, and cardiac fibrosis in mice with HFpEF. **A** Schematic diagram for evaluating cardiac function and cardiac remodeling in *Fgf21*^{Adipoq} mice and *Fgf21*$^{F/F}$ controls with or without HFpEF. **B** Average systolic blood pressure (SBP, left) and diastolic blood pressure (DBP, right) of *Fgf21*^{Adipoq} and *Fgf21*$^{F/F}$ mice with or without HFpEF. $n = 5$ mice per

condition. **C** The body weight of mice mentioned above. $n = 5$ mice per condition. **D** Left ventricular systolic function. Top, representative M-mode echocardiographic tracings. Bottom, quantification of left ventricular ejection fraction (LVEF) and left ventricular fractional shortening (LVFS). $n = 5$ mice per condition. **E** Left ventricular diastolic function. Top, representative pulsed-wave Doppler (top) and tissue Doppler (bottom) tracings. Bottom, quantification of the ratio between the mitral E wave and A wave (E/A), and the mitral E wave and E′ wave (E/E′). $n = 5$ mice per condition. **F-H** The lung weight to tibia length ratio (LW/TL, **F**), running distance during exercise exhaustion test (**G**), and the heart weight to tibia length ratio (HW/TL, **H**) of mice mentioned above. $n = 5$ mice per condition. **I** Hematoxylin and eosin (H&E) and wheat germ agglutinin (WGA) staining of cardiac sections (left) and cardiomyocyte cross-sectional quantification (right) of $Fgf21^{Adipoq}$ mice and $Fgf21^{F/F}$ mice with or without HFpEF. Scale bars, 1 mm (H&E), and 25 μm (WGA). $n = 50$ cardiomyocytes per condition. **J** Cardiac mRNA expression levels of hypertrophic markers (*Anp*, *Bnp*, and *Myh7*). $n = 5$ mice per condition. **K** Dihydroethidium (DHE) staining of cardiac sections (left) and quantification of the intensity (right). Scale bars, 100 μm. $n = 5$ mice per condition. **L** Sirius red staining (left) and quantification of fibrotic areas (right). Scale bars, 50 μm. $n = 5$ mice per condition. **M** Cardiac contents of fibrotic factors (fibronectin, collagen I, and α-SMA) were tested by immunoblot. $n = 5$ mice per condition. Violin plots in **I** are presented as lines indicating the median and interquartile range; other bar graphs are presented as mean ± SEM. Statistical significance was determined by the two-way ANOVA, followed by Tukey's multiple comparison test.

Supplementary Figure 3

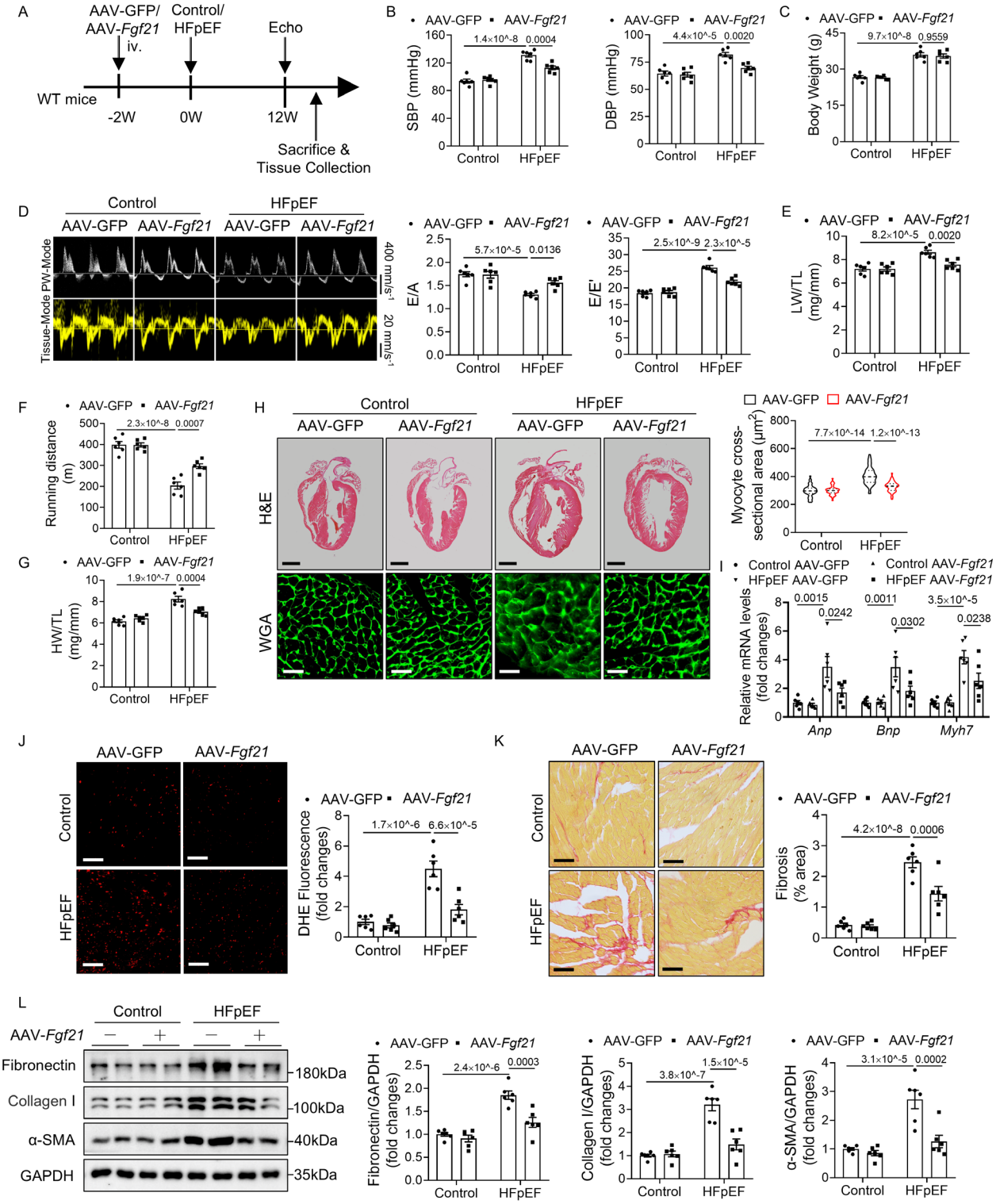

Supplementary Figure 3. AAV-*Fgf21* improves cardiac diastolic function and reduces myocyte size, oxidative stress and cardiac fibrosis in HFpEF mice. **A** Schematic diagram for evaluating AAV-*Fgf21*-treated effects in mice with HFpEF. **B** Average systolic blood pressure (SBP, left) and diastolic blood pressure (DBP, right) of mice with HFpEF after treatment with AAV-*Fgf21* or AAV-GFP. $n = 6$ mice per condition. **C** The body weight of the mice mentioned above. $n = 6$ mice per condition. **D** Left ventricular diastolic function of the mice mentioned above. Left, representative pulsed-wave Doppler (top) and tissue Doppler (bottom) tracings; Right, quantification of the ratio between the mitral E wave

and A wave (E/A), and the mitral E wave and E′ wave (E/E′). $n = 6$ mice per condition. **E**-**G** The lung weight to tibia length ratio (LW/TL, **E**), running distance during exercise exhaustion test (**F**), and the heart weight to tibia length ratio (HW/TL, **G**) of the mice mentioned above. $n = 6$ mice per condition. **H** Hematoxylin and eosin (H&E) and wheat germ agglutinin (WGA) staining of cardiac sections (left) and cardiomyocyte cross-sectional quantification (right). Scale bars, 1 mm (H&E), and 25 μm (WGA). $n = 50$ cardiomyocytes per condition. **I** Cardiac mRNA expression of hypertrophic factors (*Anp*, *Bnp*, and *Myh7*). $n = 6$ mice per condition. **J** Dihydroethidium (DHE) staining of cardiac sections (left) and quantification of the intensity (right). Scale bars, 100 μm. $n = 6$ mice per condition. **K** Sirius red staining (left) and quantification of the fibrotic areas (right). Scale bars, 50 μm. $n = 6$ mice per condition. **L** Cardiac contents of fibrotic factors (fibronectin, collagen I, and α-SMA) tested by immunoblot. $n = 6$ mice per condition. Violin plots in **H** are presented as lines indicating the median and interquartile range; other bar graphs are presented as mean ± SEM. The statistical significance of differences was assessed by two-way ANOVA, followed by Tukey's multiple comparison test.

Supplementary Figure 4

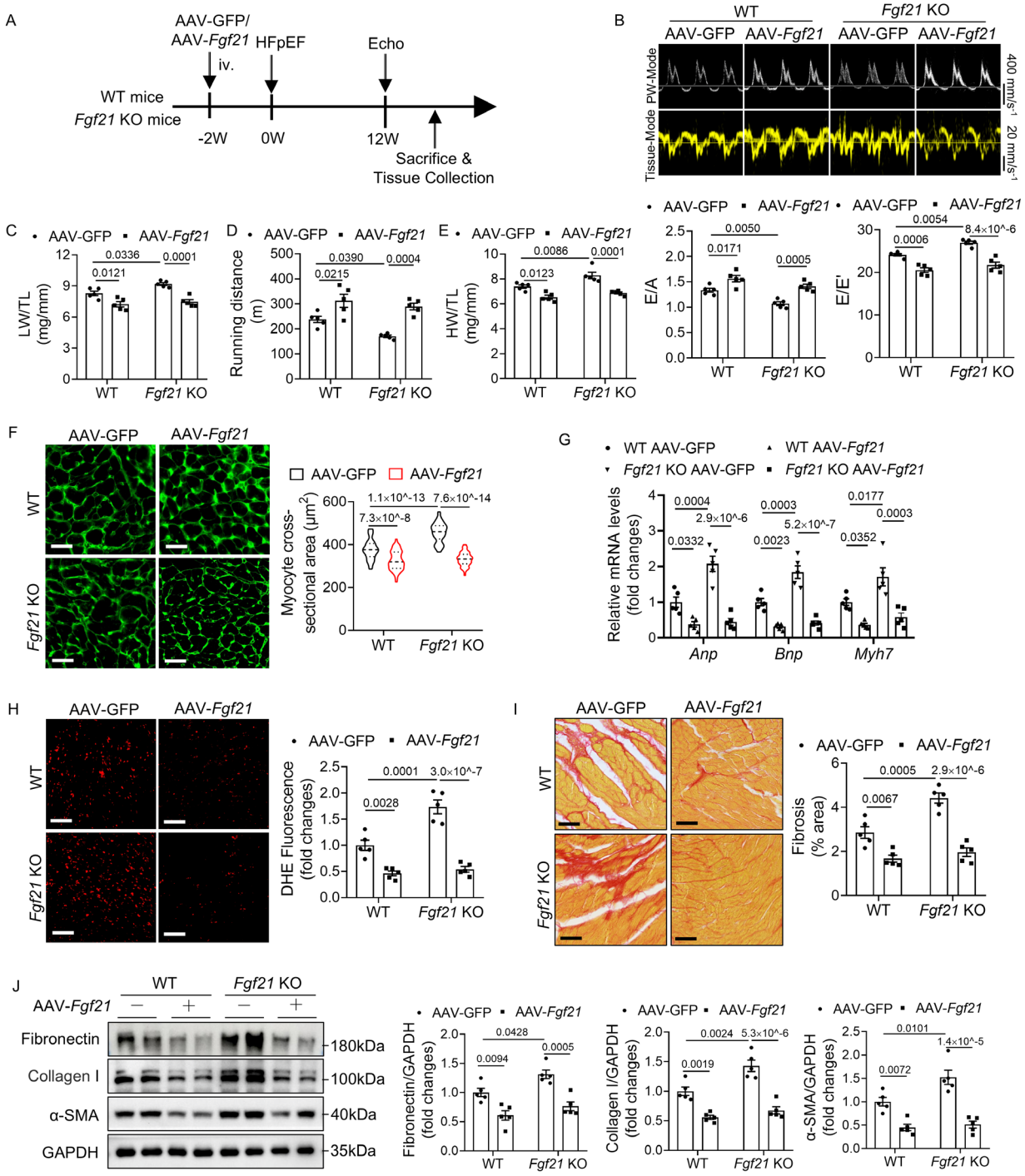

Supplementary Figure 4. Overexpression of FGF21 improves HFpEF-induced cardiac diastolic dysfunction, cardiac hypertrophy, cardiac oxidative stress and cardiac fibrosis in *Fgf21* KO mice. **A** Schematic diagram for evaluating AAV-*Fgf21*-treated effects in *Fgf21* KO mice with HFpEF. **B** Left ventricular diastolic function of *Fgf21* KO and WT mice with HFpEF after treatment with AAV-*Fgf21* or AAV-GFP, respectively. Top, representative pulsed-wave Doppler (top) and tissue Doppler (bottom) tracings; Bottom, quantification of the ratio between the mitral E wave and A wave (E/A), and the mitral E wave and E′ wave (E/E′). $n = 5$ mice per condition. **C**-**E** The lung weight to tibia length ratio (LW/TL, **C**), running distance during exercise exhaustion test (**D**), and the heart weight to tibia length ratio (HW/TL, **E**) of mice mentioned above. $n = 5$ mice per condition. **F** Wheat germ agglutinin (WGA)

staining of cardiac sections (left) and cardiomyocyte cross-sectional quantification (right). Scale bars, 25 μm. $n = 50$ cardiomyocytes per condition. **G** Cardiac mRNA expression of hypertrophic factors (*Anp*, *Bnp* and *Myh7*). $n = 5$ mice per condition. **H** Dihydroethidium (DHE) staining of cardiac sections (left) and quantification of the intensity (right). Scale bars, 100 μm. $n = 5$ mice per condition. **I** Sirius red staining (left) and quantification of the fibrotic areas (right). Scale bars, 50 μm. $n = 5$ mice per condition. **J** Cardiac contents of fibrotic factors (fibronectin, collagen I, and α-SMA) tested by immunoblot. $n = 5$ mice per condition. Violin plots in **F** are presented as lines indicating the median and interquartile range; other bar graphs are presented as mean ± SEM. The statistical significance of the differences was assessed by two-way ANOVA, followed by Tukey's multiple comparison test.

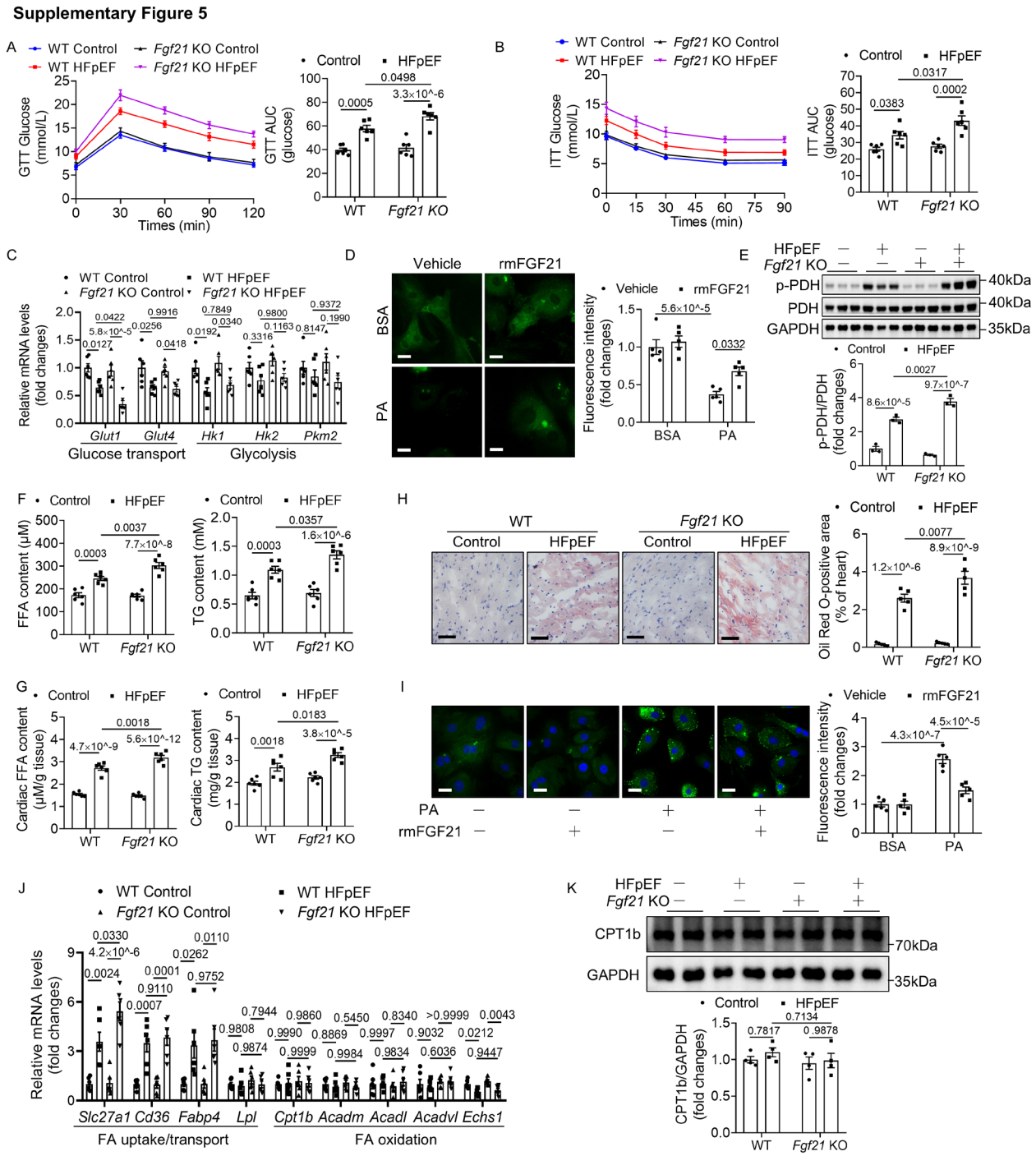

Supplementary Figure 5. The effects of FGF21 deficiency on glucose and lipid metabolism in HFpEF mice. **A** Glucose tolerance test (GTT) with incorporated area under the curve (AUC) of *Fgf21* KO and WT mice with or without HFpEF. $n = 6$ mice per condition. **B** Insulin tolerance test (ITT) with incorporated AUC of *Fgf21* KO and WT mice with or without HFpEF. $n = 6$ mice per condition. **C** Cardiac mRNA expression levels of glucose metabolism-related genes (*Glut1*, *Glut4*, *Hk1*, *Hk2*, and *Pkm2*). $n = 6$ mice per condition. **D** and **I** Neonatal rat ventricular myocytes (NRVMs) were exposed to palmitic acid (PA) with a dosage of 500 μmol/L, then incubated with recombinant mouse FGF21 (rmFGF21) for 24 hours. **D** Representative images of 2-NBDG staining (left) and quantification of the 2-NBDG intensity (right). Scale bar, 20 μm. $n = 5$ biological samples. **E** Cardiac p-PDH and PDH contents of mice tested by immunoblot. $n = 3$ mice per condition. **F** Serum free fatty acids (FFA, left)

and triglyceride (TG, right) levels in *Fgf21* KO and WT mice with or without HFpEF. $n = 6$ mice per condition. **G** Cardiac FFA (left) and TG levels (right) in *Fgf21* KO and WT mice with or without HFpEF. $n = 6$ mice per condition. **H** Representative images of Oil Red O-staining (left) and quantification of the areas (right). Scale bars, 50 μm. $n = 5$ mice per condition. **I** Representative images of BODIPY staining (left) and quantification of the BODIPY intensity (right). Scale bar, 20 μm. $n = 5$ biological samples. **J** Cardiac mRNA expression levels of fatty acid metabolism-related genes (*Slc27a1*, *Cd36*, *Fabp4*, *Lpl*, *Cpt1b*, *Acadm*, *Acadl*, *Acadvl* and *Echs1*). $n = 6$ mice per condition. **K** Cardiac CPT1b contents of mice tested by immunoblot. $n = 4$ mice per condition. Data are presented as mean ± SEM. Statistical significance was assessed by two-way ANOVA, followed by Tukey's multiple comparison test.

Supplementary Figure 6

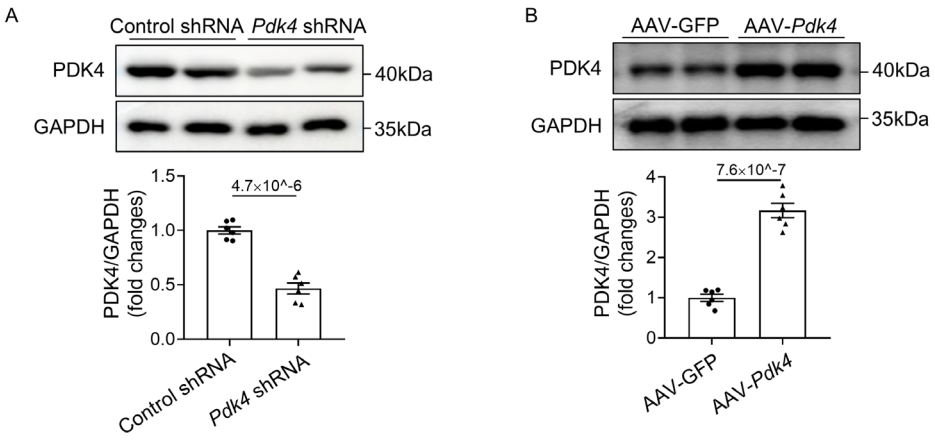

Supplementary Figure 6. Validation of *Pdk4* shRNA and AAV-*Pdk4* effectiveness.
A Cardiac PDK4 levels of mice treated with *Pdk4* shRNA or controls. $n = 6$ mice per condition. **B** Cardiac PDK4 levels in AAV-*Pdk4*- or AAV-GFP-treated mice. $n = 6$ mice per condition. Data are presented as mean ± SEM. Statistical significance was determined by the two-tailed unpaired Student's *t* test.

Supplementary Figure 7

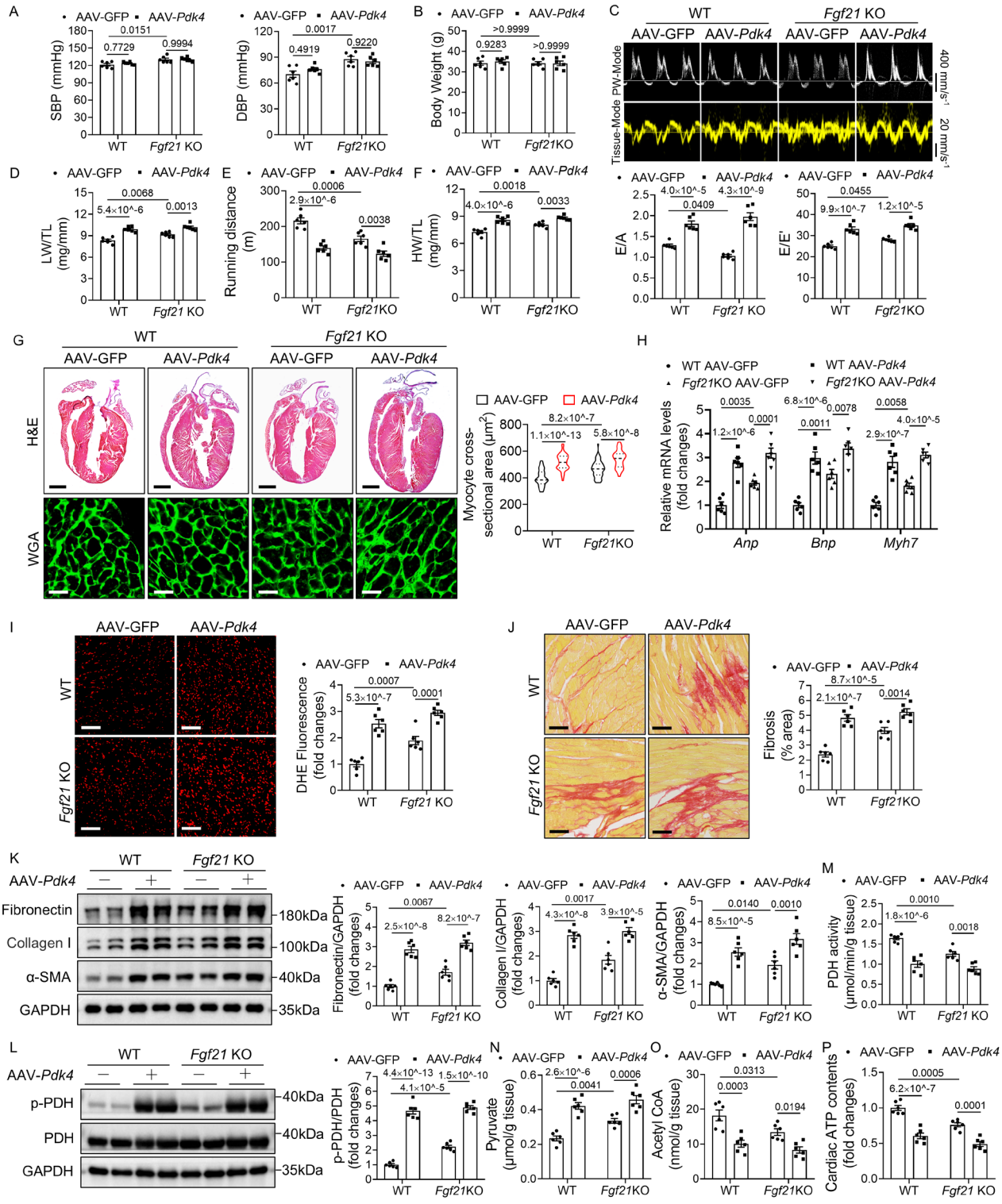

Supplementary Figure 7. Overexpression of PDK4 exacerbates HFpEF-induced cardiac diastolic dysfunction, cardiac hypertrophy, cardiac oxidative stress and cardiac fibrosis in mice. **A** Average systolic blood pressure (SBP, left) and diastolic blood pressure (DBP, right) of *Fgf21* KO and WT mice with HFpEF, treated with AAV-*Pdk4* or AAV-GFP, respectively. $n = 6$ mice per condition. **B** The body weight of the mice mentioned above. $n = 6$ mice per condition. **C** Left ventricular diastolic function of the mice mentioned above. Top, representative pulsed-wave Doppler (top) and tissue Doppler (bottom) tracings. Bottom, quantification of the ratio between the mitral E wave and A wave (E/A), and the

mitral E wave and E′ wave (E/E′). $n = 6$ mice per condition. **D** The lung weight to tibia length ratio (LW/TL) of the mice mentioned above. $n = 6$ mice per condition. **E**, **F** Running distance during exercise exhaustion test (**E**) and the heart weight to tibia length ratio (HW/TL, **F**) of the mice mentioned above. $n = 6$ mice per condition. **G** Hematoxylin and eosin (H&E) and wheat germ agglutinin (WGA) staining of cardiac sections (left) and cardiomyocyte cross-sectional area quantification (right) of the mice mentioned above. Scale bars, 1 mm (H&E), and 25 μm (WGA). $n = 50$ cardiomyocytes per condition. **H** The mRNA expression levels of cardiac hypertrophic marker genes (*Anp*, *Bnp*, and *Myh7*) in the mice mentioned above. $n = 6$ mice per condition. **I** Dihydroethidium (DHE) staining (left) of heart tissues and quantification of the intensity (right), Scale bars, 100 μm. $n = 6$ mice per condition. **J** Sirius red staining of heart tissues (left) and quantification of the fibrotic areas (right). Scale bars, 50 μm. $n = 6$ mice per condition. **K** Cardiac contents of fibrotic factors, including fibronectin, collagen I, and α-SMA tested by immunoblot. $n = 6$ mice per condition. **L** Cardiac p-PDH and PDH contents of mice tested by immunoblot. $n = 6$ mice per condition. **M** Cardiac pyruvate dehydrogenase activity in mice mentioned above. **N**-**P** Cardiac pyruvate (**N**), acetyl-CoA (**O**), and ATP (**P**) contents in mice mentioned above. $n = 6$ mice per condition. Violin plots in **G** are presented as lines indicating the median and interquartile range; other bar graphs are presented as mean ± SEM. The statistical significance of differences was assessed by two-way ANOVA, followed by Tukey's multiple comparison test.

Supplementary Figure 8

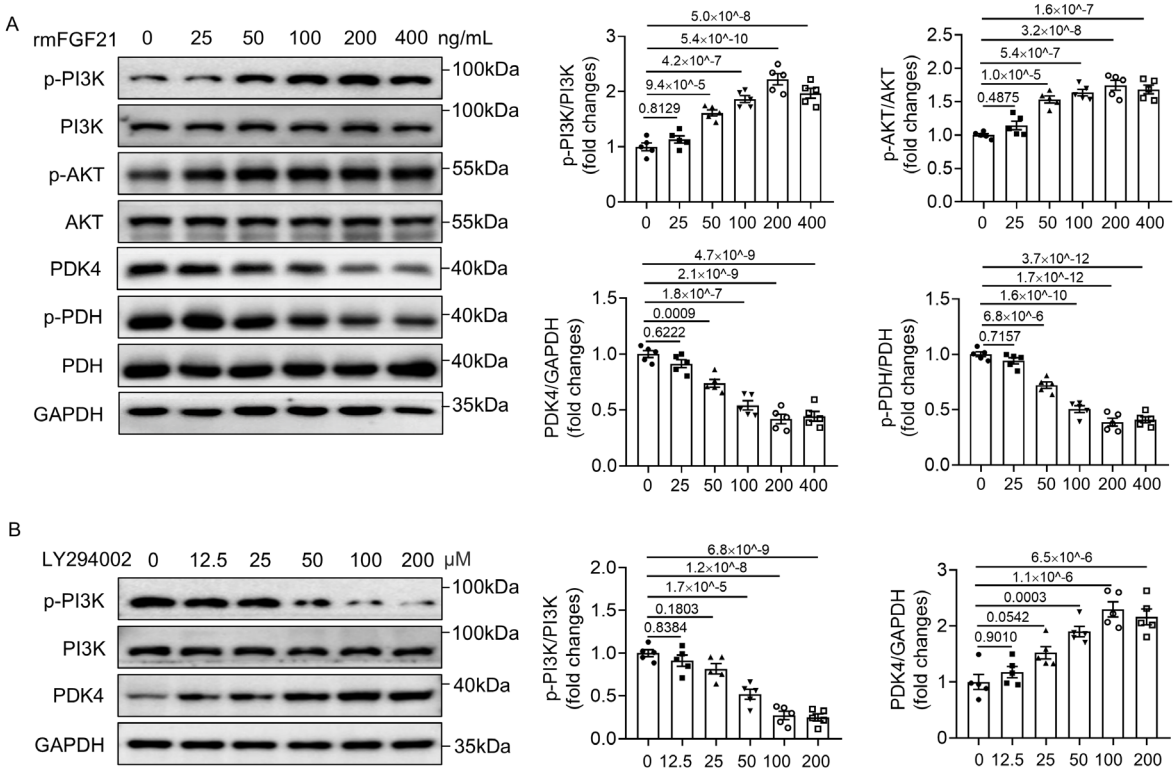

Supplementary Figure 8. FGF21 activates PI3K/AKT phosphorylation and inhibits PDK4 expression dosage-dependently. **A** Neonatal rat ventricular myocytes (NRVMs) were treated with various dosages of recombinant mouse FGF21 (rmFGF21, 0 - 400 ng/mL) for 24 hours. p-PI3K, PI3K, p-AKT, AKT, PDK4, p-PDH, and PDH were examined by immunoblot. $n = 5$ biological samples. **B** NRVMs were treated with various dosages of PI3K inhibitor LY294002 (0 - 200 μM) for 24 hours, and p-PI3K, PI3K, and PDK4 were tested by immunoblot. $n = 5$ biological samples. Data are presented as mean ± SEM. The statistical significance of differences was assessed by one-way ANOVA, followed by Tukey's multiple comparison test.

Supplementary Figure 9

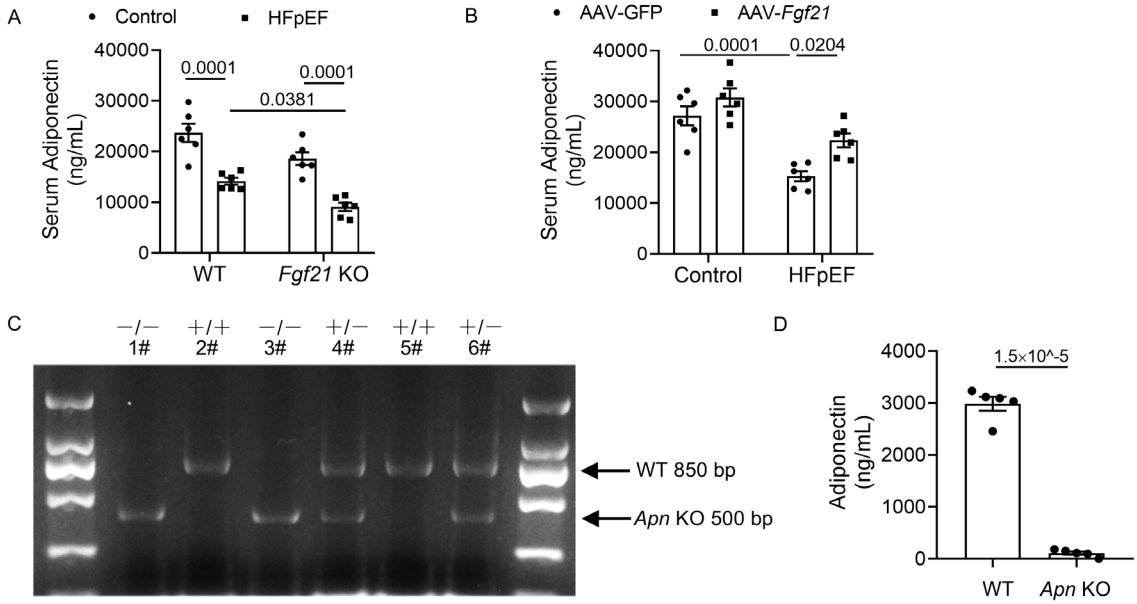

Supplementary Figure 9. Circulating adiponectin levels in FGF21 null mice with HFpEF and genotype of *Apn* KO mice. **A** Serum adiponectin levels in *Fgf21* KO and WT mice with HFpEF or controls were tested by immunoassay. $n = 6$ mice per condition. **B** Serum adiponectin levels in AAV-*Fgf21*- or AAV-GFP-treated mice with HFpEF were tested by immunoassay. $n = 6$ mice per condition. **C** Representative polymerase chain reaction (PCR) genotyping of *Apn* KO and WT littermate mice. Genotypes of mice were determined by PCR using the following primers: P1-*Apn* (5'-TGGATGCTGCCATGTTCCCAT-3'), P2-*Apn* (5'-CTTGTGTCTGTGTCTAGGCCTT-3'), and P3-*Apn* (5'-CTCCAGACTGCCTTGGGA-3'). The length of the PCR product of WT primers was 850 bp and *Apn* KO primers was 500 bp. **D** Adiponectin levels in the cultured medium were measured by immunoassay. $n = 5$ biological samples. Data are presented as mean ± SEM. Statistical analyses were performed using two-way ANOVA with the Tukey's multiple comparison test (**A**, **B**) and two-tailed unpaired Student's *t* test with Welch's correction (**D**).

Supplementary Figure 10

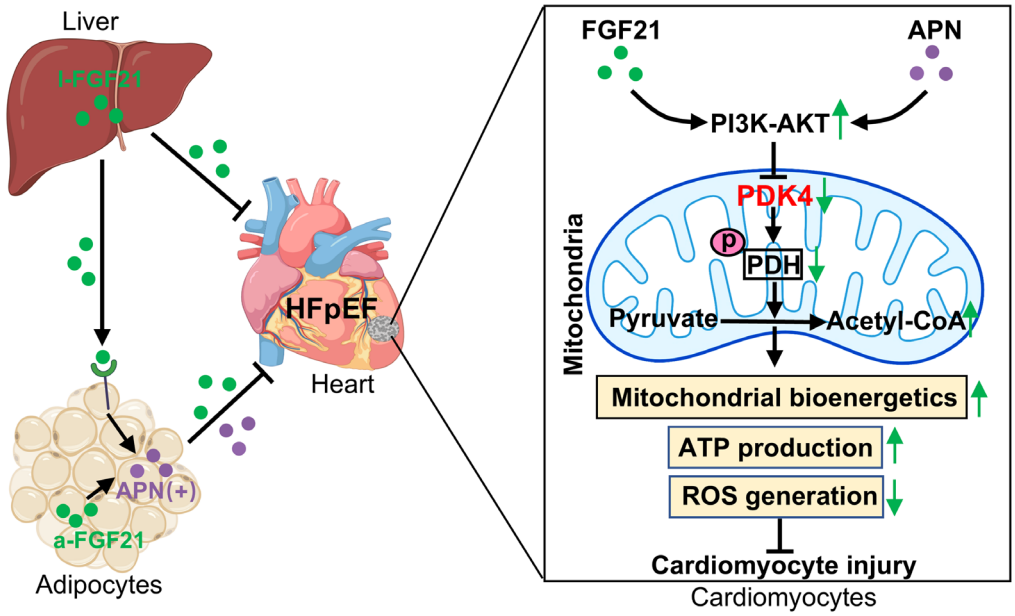

Supplementary Figure 10. Schematic view of the mechanism whereby FGF21 protects against HFpEF and its related cardiac diastolic dysfunction and damage. Mechanically, FGF21 targets adipocytes to promote the production of adiponectin, which in turn acts on cardiomyocytes to activate PI3K/AKT signals, or FGF21 directly acts on cardiomyocytes to trigger PI3K/AKT signals, then negatively regulates PDK4 production, and finally enhancing mitochondrial bioenergetics, thereby protects against HFpEF. Created in BioRender. Cao, C. (2025) https://BioRender.com/q09b588.

Supplementary Table 1. **Baseline characteristics according to FGF21 tertiles**

Variables	Tertile 1 (n = 51) 131.76 pg/mL (100.85-185.25)	Tertile 2 (n = 50) 348.79 pg/mL (289.64-413.70)	Tertile 3 (n = 50) 973.52 pg/mL (731.82-1365.80)	*p* value
Age, years	64.73 ± 14.19	66.18 ± 12.12	62.16 ± 17.16	0.382
BMI, kg/m^2	24.26 ± 3.54	25.70 ± 3.84	25.14 ± 3.95	0.161
Male, n (%)	25 (49.0)	31 (62.0)	21 (42.0)	0.127
Current smoking, n (%)	15 (29.4)	18 (36.0)	14 (28.0)	0.653
Clinical history, n (%)				
Hypertension	14 (27.5)	12 (24.0)	18 (36.0)	0.397
Diabetes mellitus	3 (5.9)	10 (20.0)	5 (10.0)	0.080
Dyslipidemia	11 (21.6)	12 (24.0)	9 (18.0)	0.761
CKD	3 (5.9)	6 (12.0)	18 (36.0)	**< 0.001**
NYHA class, n (%)				
I, n (%)	31 (60.8)	29 (58.0)	25 (50.0)	0.527
II, n (%)	16 (31.4)	14 (28.0)	9 (18.0)	0.281
III, n (%)	3 (5.9)	5 (10.0)	8 (16.0)	0.252
IV, n (%)	1 (2.0)	2 (4.0)	8 (16.0)	**0.014**
Hemodynamics				
SBP, mmHg	129.37 ± 17.08	127.26 ± 15.57	131.96 ± 28.73	0.543
DBP, mmHg	76.18 ± 12.95	74.44 ± 12.17	71.90 ± 17.14	0.320
LVEF, %	62.0 (58.0-65.8)	63.0 (57.8-66.3)	55.0 (52.0-64.0)	**0.011**
IVSd, mm	10.0 (9.0-11.0)	10.00 (9.0-12.0)	11.0 (9.0-13.0)	0.262
LVEDV, ml	49.0 (45.0-53.0)	47.0 (42.8-54.5)	50.0 (45.0-53.0)	0.729
Laboratory data				
BNP, pg/mL	164.0 (74.3-296.0)	423.5 (254.0-600.5)	554.0 (234.0-1093.0)	**< 0.001**
TG, mmol/L	1.03 (0.79-1.53)	0.99 (0.74-1.55)	1.18 (0.83-1.59)	0.853
TC, mmol/L	4.10 (3.51-4.82)	3.67 (2.90-4.26)	3.87 (3.05-4.47)	0.059
HDL-c, mmol/L	1.22 (1.04-1.52)	1.05 (0.94-1.20)	0.95 (0.78-1.23)	**< 0.001**
LDL-c, mmol/L	2.25 (1.78-2.98)	2.07 (1.36-2.57)	2.18 (1.72-2.91)	0.104
Scr, mg/dL	74.15 (59.33-92.03)	81.35 (66.63-104.53)	115.30 (69.70-314.30)	**0.001**
FPG, mmol/L	5.15 (4.45-5.91)	5.75 (4.94-7.02)	5.75 (5.13-7.21)	**0.008**

Abbreviations: BMI, body mass index; CKD, chronic kidney disease; NYHA, New York Heart Association; SBP, systolic blood pressure; DBP, diastolic blood pressure; LVEF, left ventricular ejection fraction; IVSd, interventricular septum depth; LVEDV, left ventricular end-diastolic volume; BNP, brain natriuretic peptide; TG, triglyceride; TC, total cholesterol; HDL-c, high-density lipoprotein cholesterol; LDL-c, low-density lipoprotein cholesterol; Scr, serum creatinine; FPG, fasting plasma glucose. Statistical analysis was performed using ANOVA with the multiple-comparisons test with Bonferroni correction and the Kruskal-Wallis test.

Supplementary Table 2. Correlation between circulating levels of FGF21* with various anthropometric and biochemical parameters in patients with HFpEF (n = 151)

Variables	Serum FGF21	
	r	*p*
Age	-0.131	0.108
Sex	0.045	0.498
BMI	0.077	0.347
SBP	0.065	0.429
DBP	-0.124	0.13
LVEF	-0.204	**0.013**
LVFS	-0.111	0.256
IVSd	0.104	0.229
LVEDV	-0.034	0.681
BNP*	0.541	**< 0.001**
FPG*	0.149	0.068
TG*	0.012	0.882
TC*	-0.167	0.042
HDL-c*	-0.307	**< 0.001**
LDL-c*	-0.024	0.769
Scr*	0.284	**< 0.001**
Current smoking	0.01	0.879
Hypertension	0.055	0.413
Diabetes mellitus	0.049	0.466
Dyslipidemia	-0.024	0.719
CKD	0.273	**< 0.001**

*Log transformed before analysis.

Pearson correlation coefficient for a continuous variable and Kendall tau-b correlation coefficient for categorical variable were used to analyze the associations between cardiac function parameters and serum levels of FGF21 (log-transformed as required).

Supplementary Table 3. Primers used for the RT-qPCR assays in this study

Gene	Forward primers (5'- 3')	Reverse primers (5'- 3')
Anp	GGGTAGGATTGACAGGATTGG	CTCCTTGGCTGTTATCTTCGG
Bnp	TGGGAGGTCACTCCTATCCT	GGCCATTTCCTCCGACTTT
Myh7	AGACTGTCAACACTAAGAGGGT	TGCCCCAAAATGGATTCGGAT
Glut1	GCTTCTCCAACTGGACCTCAAAC	ACGAGGAGCACCGTGAAGATGA
Glut4	CCTGCCCGAAAGAGTCTAAAG	CTCTCTCTCCAACTTCCGTTTC
Hk1	TCCATCCACACTTCTCCAGAATC	GATCCTGGCTCTTAGGCGTTC
Hk2	TCATTGTTGGCACTGGAAGC	TTGCCAGGGTTGAGAGAGAG
Pkm2	ATTATTTGAGGAACTCCGCCGCCT	ATTCCGGGTCACAGCAATGATGG
Slc27a1	CTGCCAAGGCCCTCATTTA	CAGATCTCCAGAGCAGAACTTG
Cd36	CCTCCAGAATCCAGACAACC	CACAGGCTTTCCTTCTTTGC
Fabp4	GAGCACCATAACCTTAGATGGG	CCACCAGTTTATCATCCTCTCG
Lpl	AGAGAGGACTCGGAGACGTG	GGAGTTGCACCTGTATGCCT
Cpt1b	TGGCTGAGGTACTTTCTGAACC	AGAGACCCCGTAGCCATCAT
Acadm	GCTAGTGGAGCACCAAGGAG	CCAGGCTGCTCTCTGGTAAC
Acadl	TTTCCGGGAGAGTGTAAGGA	ACTTCTCCAGCTTTCTCCCA
Acadvl	GCTCTGCAAGGCTGTATGGA	CGATTCCTGTCCTCCGTCTC
Echs1	CCAGTTCGGACAGCCAGAAA	ACAAGACCTGCCTGCTTTGC
Gapdh	GCACAGTCAAGGCCGAGAAT	GCCTTCTCCATGGTGGTGAA